Ann. Occup. Hyg.

doi:10.1093/annhyg/met041

Development of a Sampler to Estimate Regional Deposition of Aerosol in the Human Respiratory Tract

KIRSTEN A. KOEHLER* and JOHN VOLCKENS

Department of Environmental Health Sciences, Johns Hopkins Bloomberg School of Public Health, 615 N Wolfe Street, Baltimore, MD 21205, USA

Received 15 March 2013; in final form 13 June 2013; accepted 13 June 2013

A multistage sampler was developed and tested to estimate regional deposition of aerosol in the human respiratory system. The motivation for this research is to improve our ability to estimate inhaled aerosol dose. Current methods for aerosol measurement and exposure/risk assessment are based on particle aspiration (e.g. inhalable PM) or on penetration to various regions of the respiratory system (e.g. PM_{10}). The sampler developed here operates at 1 m^3 h^{-1} (16.7 l min^{-1}) of flow and utilizes several substrates, connected in series, to mimic regional particle deposition. Two sets of polyurethane foam substrates are used to mimic particle deposition in the head airways and tracheobronchial regions, respectively. Particle deposition in the alveolar region is mimicked using diffusion screens. These substrates are amenable to trace chemical analyses but not gravimetric analyses, due to water vapor uptake with small changes in relative humidity.

Keywords: aerosols; endotoxin; exposure assessment

INTRODUCTION

Particle size distribution plays a major role in determining both the inhaled dose and the region affected by aerosol hazards (Johnson and Esmen, 2004). As such, there has been increasing interest in estimating the deposition of particles in the respiratory system, as opposed to assessing aerosol exposure (i.e. total particulate mass) or any of the various particle penetration metrics (e.g. inhalable, thoracic, and respirable fractions). The International Organization for Standardization (ISO) has developed standards for respiratory deposition based on proposed conventions (Bartley and Vincent, 2011; ISO/CEN, 2012). The deposited fraction of particles in the respiratory system is often estimated by measuring or modeling the full particle size distribution using various direct-reading or integrated techniques (e.g. scanning mobility particle sizer or multistage impactor) and then inferring deposited fractions from the size distribution data (Kelly *et al.*, 2011). Other researchers have developed samplers to estimate aerosol deposition in the lung directly. For example, Kuo *et al.* (2005) developed a size-selective sampling inlet to mimic the International Commission on Radiological Protection (ICRP, 1994) convention for total deposition. However, the inlet for this device removed virtually all particles with $d_{ae} > 0.8$ μm and thus greatly underestimated the contribution from supermicron aerosol. Cena *et al.* (2011) described a personal nanoparticle respiratory deposition sampler that used an impactor to remove particles >0.3 μm and diffusion screens to mimic the total deposition fraction for nanoparticles.

In our previous work, we employed a semi-empirical model to design an aerosol sampler made from porous, polyurethane foam to reproduce the size-specific (but not region-specific) deposition of aerosol in the human respiratory system (Koehler *et al.*, 2009). Although the total deposition sampler provides a better estimate of aerosol dose than penetration-based samplers, the total deposition sampler does not give any indication

*Author to whom correspondence should be addressed.
Tel: +410-955-7706; fax: +410-955-9334;
e-mail: kirsten.koehler@colostate.edu

of where particles deposit in the respiratory system. Regional deposition can influence the incidence of certain health outcomes (e.g. sinusitis versus bronchitis versus pneumonia). Particles that deposit in the head airways and tracheobronchial region are ultimately swallowed (the latter via mucociliary clearance), whereas particles that deposit in the alveolar region may have long half-lives within the lungs. Distinguishing where particle deposition occurs may improve our understanding of the pathways by which particles cause disease.

This work describes the development of an aerosol sampler to mimic regional particle deposition in the human respiratory tract. The ICRP has developed a model that estimates particle deposition, as a function of particle aerodynamic or thermodynamic diameter, in three main regions of the respiratory tract: the head airways, tracheobronchial, and alveolar regions. We have used the simplified deposition models described by Hinds (1999) based on the ICRP Deposition Model for the average of adult males and females under three exercise conditions (hereafter, 'ICRP convention'). We used two semi-empirical models (Cheng *et al.*, 1980; Clark *et al.*, 2009) to design substrates capable of matching the ICRP-defined deposition to these regions. These substrates, made from polyurethane foam and nylon mesh screen, have specific dimensions (i.e. length, diameter, and fiber size) and operating conditions (e.g. face velocity) necessary to reproduce size-specific particle deposition in the human respiratory tract. The substrates were placed in series within a sample holder that operated at 16.7 l min^{-1} of flow. Performance of the regional deposition sampler (RDS) was evaluated using test aerosols ranging in size from 0.01 to 10 µm.

METHODS

Sampler design

The penetration, P, of aerosol through a foam plug is given by

$$\ln(P) = -\frac{t}{d_f}\{40.7\mathrm{St}^{1.9} + 38.9\mathrm{Ng}^{0.88} + 84.4\mathrm{Pe}^{-0.75}\}, \quad (1)$$

where t is the thickness of the foam plug (in millimeter), d_f is the diameter of a typical foam fiber (in micrometer), and St, Ng, and Pe represent the Stokes number, the gravitational settling number, and the Peclet number, respectively (Kenny *et al.*, 2001; Clark *et al.*, 2009). Each dimensionless number describes the tendency of a particle to deposit within the foam due to inertial impaction (St), gravity (Ng), or diffusion (Pe). They are quantified by the following equations:

$$\mathrm{St} = \frac{\rho_0 d_{ae}^2 U C_C}{18\eta d_f}, \quad (2)$$

$$\mathrm{Ng} = \frac{\rho_p d_{ae}^2 g C_C}{18\eta U}, \quad (3)$$

$$\mathrm{Pe} = \frac{3\pi\eta d_{th} d_f U}{kTC_C}, \quad (4)$$

where d_{ae} is the particle aerodynamic diameter, d_{th} is the thermodynamic diameter, ρ_0 is standard density (i.e. the density of water), η is the viscosity of air, U is the face velocity of air through the foam, C_c is the Cunningham slip correction factor, d_f is the fiber diameter, g is the acceleration due to gravity, k is Boltzmann's constant, and T is temperature in kelvin. All units are in SI.

The foam deposition model (where deposition = 1 − penetration) described by equation (1) was used to find foam and flow characteristics (foam fiber diameter, thickness, and face velocity) to best match the regional deposition of aerosol in the respiratory system according to the ICRP convention. The deposition of aerosol through the first foam was calculated from equation (1) and (for modeling purposes) the deposition through subsequent foams is based only on the proportion of aerosol that penetrated through the previous foams. Two pieces of foam were required to match deposition in the head airways and two more for the tracheobronchial (four total). All foam inserts must be operated in series for proper regional deposition estimates. Foam properties for the head airways and tracheobronchial regions are listed in Table 1 and the regional deposition is compared to the ICRP convention in Fig. 1.

Because the foam deposition model suggested unreasonable foam properties (thickness and face velocity) for alveolar deposition, we chose to mimic alveolar deposition using diffusion screens similar to those used by Cena *et al.* (2011). The deposition of particles in the screens was predicted using the diffusion screen deposition model described by Cheng *et al.* (1980).

$$\log(P) = -n(1.96\mathrm{Pe}^{-(2/3)} + 1.69 f(R) + 3.91 I \cdot \mathrm{St} + 1.94\mathrm{Pe}^{-(1/2)} R^{2/3}), \quad (5)$$

Table 1. Substrate dimensions and operating conditions for the RDS.

Stage	Respiratory region	Insert diameter (cm)	Insert length (cm)	Fiber diameter (μm)	Face velocity (m s^{-1})
1 (foam)	Head airways	0.8	4.6	92	5.50
2 (foam)	Head airways	4.0	0.6	92	0.22
3 (foam)	Tracheobronchial	1.15	4.4	126	2.64
4 (foam)	Tracheobronchial	1.75	5.0	126	1.10
5 (nylon mesh)	Alveolar	9	4 layers	6	0.043

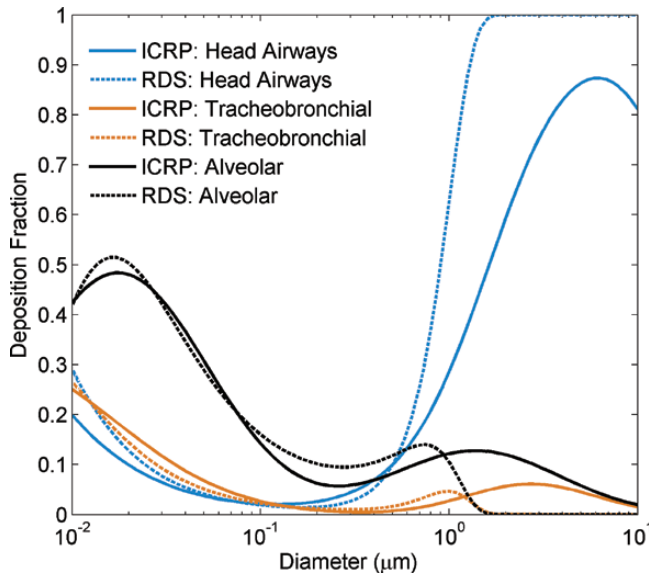

Fig. 1. Modeled deposition fractions (ICRP and RDS sampler) as a function of particle diameter (calculated from equations 1 and 5) for each of three regions in the human respiratory tract (color version available online).

where n is the number of screens, R is the interception diameter (d_{ae}/d_f), $f(R) = (1 + R)^{-1} - (1 + R) + 2(1 + R)\ln(1 + R)$, $I = (29.6 - 28\alpha^{0.62})R^2 - 27.5R^{2.8}$, and α is the solid volume fraction of the screen (0.89 for nylon mesh). The nylon mesh properties used for the alveolar deposition are listed in Table 1 and the deposition is compared to the ICRP alveolar deposition in Fig. 1.

Foam inserts and the nylon mesh screens each require distinct face velocities to generate the appropriate size-dependent deposition. To achieve a constant flow rate through the entire assembly, the diameters of the foam inserts and nylon mesh screens were calculated to achieve the proper face velocity at volumetric flow of 1 $m^3\ h^{-1}$ (16.7 l min^{-1}). Consequently, a very large nylon mesh screen diameter was required to increase the residence time through the screens, allowing for diffusional deposition of particles <0.1 μm and to minimize the deposition of larger particles via impaction. A computer-aided design drawing of the RDS is shown in Fig. 2.

Sampler evaluation

Validating foam and screen deposition fractions. Several experiments were conducted with the engineered substrates (foam and nylon screens) to assess performance and reliability. First, we evaluated the diffusion screen deposition model with two nylon mesh pore sizes (11 and 20 μm, Millipore Part No. NY1109000) operating at two face velocities (0.13 and 0.19 m s^{-1}) and compared to modeled deposition values from Cheng *et al.* (1980). Next, we tested the particle deposition efficiency of each foam substrate and compared the measured and modeled deposition values. (equation 1). Briefly, a substrate was fit within an appropriate housing and high molecular weight oil aerosol was drawn through the substrate

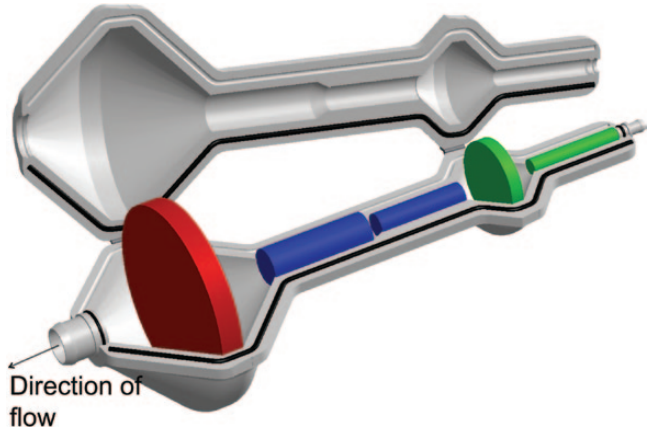

Fig. 2. Computer-aided design drawing of the RDS holding two foam inserts to match the deposition in the head airways (first two substrates), two foam inserts to match the deposition in the tracheobronchial region (next two substrates), and nylon mesh screens to match the deposition in the alveolar region (last substrate).

to determine particle penetration fraction as a function of size, similar to Clark *et al.* (2009). The penetration fraction for a given particle size, P_i, was calculated by

$$P_i = \frac{C_{i\,\text{foam+housing}}}{C_{i\,\text{housing}}}, \tag{6}$$

where $C_{i\ \text{housing}}$ is the aerosol number concentration passing through the tubing section or filter holder without foam and $C_{i\ \text{foam+housing}}$ is the aerosol number concentration after passing through the tubing section or nylon net holder with the substrate in place; all values are specific to i, which denotes the particle size. Particles with $0.01 \le d_{\text{th}} \le 1.0$ µm were sized and counted with a Sequential Mobility Particle Sizer (SMPS, GRIMM Technologies, Inc.). Particles with $0.50 \le d_{\text{ae}} \le 20$ µm were sized and counted with a TSI Aerodynamic Particle Sizer (APS, Model 3321). Only liquid aerosol was tested because previous work has shown that the size-dependent deposition does not vary with phase (solid or liquid) for sizes between 0.01 and 10 µm (Clark *et al.*, 2009; Koehler *et al.*, 2009).

Laboratory testing of mass-based deposition measurements. Next, we tested the ability of the RDS to estimate the mass of aerosol deposited in each respiratory region. Gravimetric analysis is problematic with foam inserts due to the foam hygroscopicity (Koehler *et al.*, 2009). Instead, we used fluorescence analysis, which is sensitive to aerosol mass on the order of nanograms (Tolocka *et al.*, 2001). Oleic acid was mixed with fluorescein powder (~1 wt%) to generate a fluorescently labeled test aerosol and nebulized in an ~1m^3 aerosol chamber. The aerosol was neutralized prior to sampling (TSI, Inc. Model 3012). Two RDSs sampled the test aerosol in parallel to determine the fraction of mass deposited in each region and to estimate variability between samplers. Two different test aerosols, each of different size distribution, were evaluated: one with a larger mass median diameter (MMD) representative of a mechanically generated aerosol and the other with a smaller MMD representative of a combustion-generated aerosol.

The reference aerosol mass distribution was established with a Nano-MOUDI II cascade impactor (MSP Model 125B). A 47-mm diameter Teflon-coated glass fiber filter (Pallflex, Pall Inc.) was placed in each impactor stage. Aerosol size distribution was also monitored continuously during the experiment using SMPS and APS instruments. Aerosol mass concentrations varied by <10% during each experiment.

For measurements of fluorescently labeled particles, collected aerosol mass was extracted and then quantified by excitation–emission spectroscopy. To determine fluorescent mass, each impactor substrate was placed in a 15-ml centrifuge tube and extracted with 4 ml of 3% ammonium hydroxide solution. Foam extractions for stages 1 and 3 were completed in 15-ml centrifuge tubes with 8 ml of extraction solution. Foam inserts for stages 2 and 4 were placed in 60-ml centrifuge tubes (to accommodate the insert diameters) and extracted with 10 ml of extraction solution. All four nylon screens were extracted together

in a 60-ml centrifuge tube with 10 ml of extraction solution. A backup filter (47 mm diameter, Pallflex) was placed downstream of the RDS to capture the remaining aerosol (i.e. the fraction that would be exhaled) and to complete a mass balance for comparison purposes. This filter was placed in a 15-ml centrifuge tube and extracted in 4 ml of extraction solution. All filters were sonicated for 10 min to ensure efficient extraction. Foam substrates were sonicated for 60 min and then placed on a shaker table for 1 h. Three aliquots of 200 µl (i.e. triplicate samples) were taken from each extract, pipetted into 96-well plates, and analyzed in a fluorescence plate reader (FLX-800, BioTek Inc., Winooski, VT). Results are reported in relative fluorescence units (RFU), which is a reliable surrogate for mass. Serial dilutions of calibration standards were analyzed to ensure linearity of the fluorescence signal over the range of concentrations sampled. The limit of quantification for the fluorescence measurements was 10 RFU, corresponding to ~0.5 ng of fluorescein per sample.

Using the midpoint diameter of each Nano-MOUDI size bin, we estimated the fraction of mass that would deposit in each region of the respiratory system from the ICRP model and by the RDS sampler deposition model (equations 1 and 5). The ICRP and RDS deposition model fractions were multiplied by the measured mass fraction in each size bin and summed over all Nano-MOUDI stages to determine the fraction depositing in each respiratory region. The calculated deposition fraction in each region was compared to the measured mass in each stage of the RDS (i.e. the masses measured in foam inserts 1 and 2 were summed to estimate the deposition in the head airways region, the masses measured in foam inserts 3 and 4 were summed to estimate the deposition in the tracheobronchial region, and the masses measured in all four screens estimated the deposition in the alveolar region).

Field testing of RDS. Finally, we evaluated whether the RDS could estimate regional deposition of endotoxin in a real-world environment (an animal holding facility). The RDS (16.7 l min^{-1}) and a PM_{10} (Personal Environmental Monitor, SKC, Inc., 4 l min^{-1}) sampler with a 37-mm Pallflex filter were co-located in an animal pavilion located on the Colorado State University campus. No animals were present in the pavilion during the measurement, so a leaf blower was used to resuspend settled dust (simulating a common clean-up activity for this facility). Aerosol samples were collected for 4 h from a highly variable mass concentration with an average PM_{10} concentration of 35 µg m^{-3} as measured by an aerosol nephelometer (Dustrak Model 8520, TSI, Inc.). Foam inserts and the PM_{10} filter were stored in centrifuge tubes and frozen until analysis. Each sample was extracted with 10 ml of 0.05% polysorbate 20 (Tween) solution, sonicated for 1 min, followed by shaking for 1 h at 37°C. Endotoxin analysis was performed using a PyroGene Recombinant factor C endotoxin assay (Lonza Inc., Walkersville, MD). Endotoxin assays on substrate blanks were below the limit of detection for all substrates.

RESULTS

Validation of RDS substrates

Engineered foam inserts. The size-specific deposition of aerosol through each foam insert is shown in Fig. 3a–d. Each point represents the average of three replicates and the error bars represent 1 SD. The blue line represents the predicted deposition through the individual foam as calculated by the foam deposition model (equation 1). Good agreement was observed between the deposition measured through the foam substrates and the foam deposition model. Many of the foams exhibit higher deposition fractions than predicted for particles >2 µm. However, the enhanced deposition of larger sized particles will result in a positive bias of the sampling efficiency of the first foam insert since the collection efficiency is near 100% and those particles will not penetrate further downstream, which may result in underestimation of mass in subsequent foam inserts.

Nylon mesh screens. The diffusion screen deposition model (equation 5), based on single-fiber filtration efficiency, required some tuning to accurately predict deposition through commercially available nylon mesh (Millipore, NY1109000). Preliminary testing of the size-specific deposition of aerosol through the nylon mesh at different face velocities and for different pore sizes was completed in a similar way as described in Sampler design. The manufacturer only provided the pore size, not the fiber diameter as required for equation (5). We found that for the nylon mesh, using a fiber diameter equal to approximately half the pore diameter reported by the manufacturer, resulted in good agreement with measured deposition. Thus,

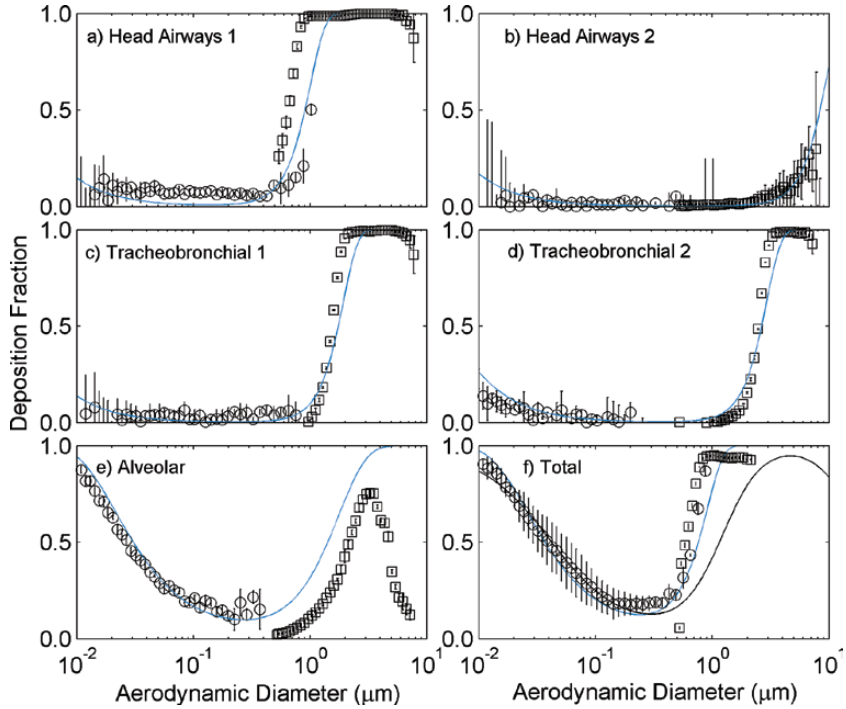

Fig. 3. Measured and modeled particle deposition fractions for each RDS substrate: (a) head airways 1; (b) head Airways 2; (c)tracheobronchial 1; (d) tracheobronchial 2; (e) alveolar. The total deposited fraction (panel f) for the entire RDS is compared to the modeled deposition (blue line, equation 1 or 5) and ICRP total deposition (black line). Open circles represent SMPS data and open squares represent APS data. Error bars represent 1 SD (color version available online).

for a nylon mesh with a manufacturer reported pore diameter (D_f) of 11 or 20 μm, simply substituting a smaller D_f of 6 or 10 μm in equation (5), respectively, produced good agreement with measured, size-dependent deposition.

Since the nylon mesh screens were only available in three diameters (25, 47, and 90 mm), and the flow rate through the RDS was constrained by the conditions necessary for the foam inserts, we inverted equation (5) using a solver algorithm to select an appropriate pore size and number of nylon mesh screens to use in the RDS. The deposition through four layers of 90-mm nylon mesh screens with a fiber diameter of 11 μm is shown in panel (e). The blue line represents the predicted deposition through the net as calculated by the diffusion screen deposition model (equation 5). Good agreement with the predicted deposition was observed for particles with diameter <0.4 μm, but the model does not accurately represent the deposition of supermicron particles. However, these larger particles are predominantly removed by upstream stages (representing deposition in the head airways and tracheobronchial regions) and contribute only a small bias to alveolar deposition.

The measured deposition through the entire RDS is shown in panel (f). The measured deposition is compared to the modeled deposition through the four foams and the screens (blue line) as well as to the ICRP convention for total deposition (black line). The total deposition shows some bias for particle diameters larger than ~0.8 μm. Therefore, due to the functional forms of the regional depositions for the ICRP model, summing the regional deposition fractions does not reproduce the total deposition perfectly. The observed differences between the total deposition and the full RDS are similar to those observed for the foam deposition sampler described by Clark *et al.* (2009).

Laboratory fluorescent particle analysis

Performance of the RDS (both models and measurements) is shown in Fig. 4 for two aerosol size distributions generated in the laboratory. The upper left panel of Fig. 4 contains results from a larger size distribution, expected to be more representative of a mechanically generated aerosol [MMD = 2.75 μm and geometric standard deviation (GSD) = 1.42]; the upper right panel

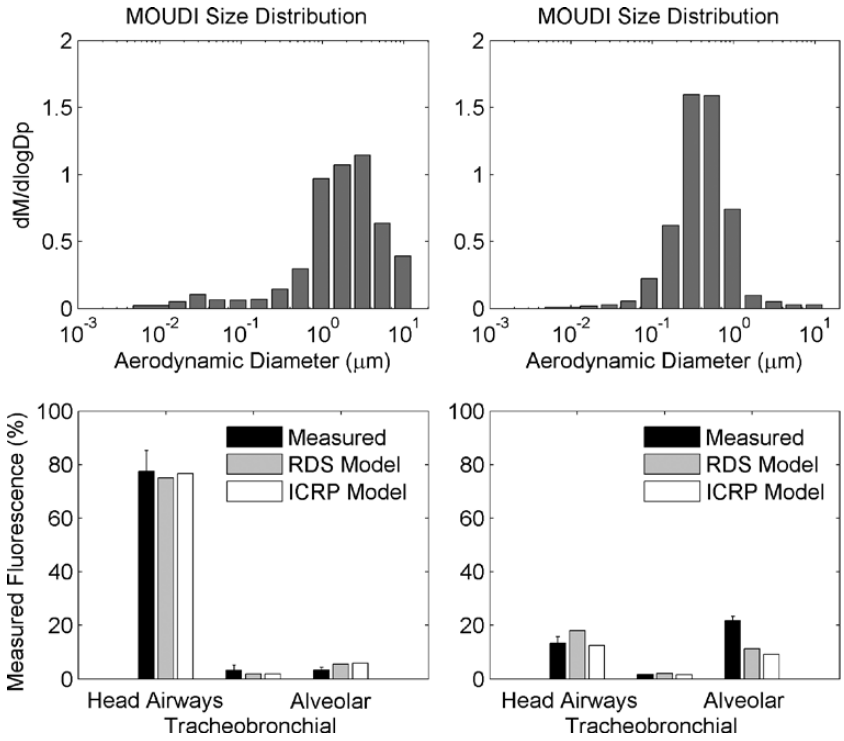

Fig. 4. Measured size distributions (top panels) and RDS performance (bottom panels) for two test aerosols generated in the laboratory. Fluorescence mass measured in each region of the RDS (black bars) is compared to RDS model predictions (equations 1 and 5, light gray bars) and ICRP model predictions for regional aerosol deposition (white bars).

contains results from a smaller size distribution, expected to be more representative of an aerosol from combustion sources (MMD = 0.31 μm and GSD = 1.48). Because these aerosols are generated from a nebulizer, the GSD is somewhat smaller than typically observed in the atmosphere (GSD > 1.5 is typical). The performance of the RDS is demonstrated in the bottom panels corresponding to each size distribution. The black bars indicate the measured percentage of particles depositing in each respiratory region according to the RDS, the gray bars represent predicted deposition from the RDS sampler model (equations 1 and 5), and the white bars represent the expected deposition in each respiratory region according to the ICRP model. Small differences in predicted deposition between ICRP and RDS models are evident; slightly larger differences are seen between modeled and measured performance.

For the large-size distribution (left panels), good agreement was found between the RDS sampler model, the ICRP model, and the RDS for all regions. Most of the aerosol deposited in the head airways with only small percentages (<10%) depositing in the tracheobronchial and alveolar regions. Larger differences were observed between the RDS and the expected deposition according to the ICRP model for the smaller size distribution in the alveolar region. This is due to the oversampling by the nylon mesh screens for sizes between 0.1 and 0.9 μm (see Fig. 1).

After accounting for differences in flow rate (9.3 l min^{-1} for the Nano-MOUDI versus 16.7 l min^{-1} for the RDS), the total fluorescence detected by the Nano-MOUDI was ~20% higher than the total fluorescence measured in the RDS (plus the backup filter). Measured losses in the RDS substrate housing were ~15%, by mass, for particle sizes between 0.02 and 0.9 μm, with the largest losses observed within the holders for the second foam insert and the nylon mesh screens because these stages have the lowest face velocities.

Endotoxin analysis

Regional deposition from a simulated endotoxin exposure (concentration of endotoxin in endotoxin units per cubic meter) is shown in Fig. 5. The

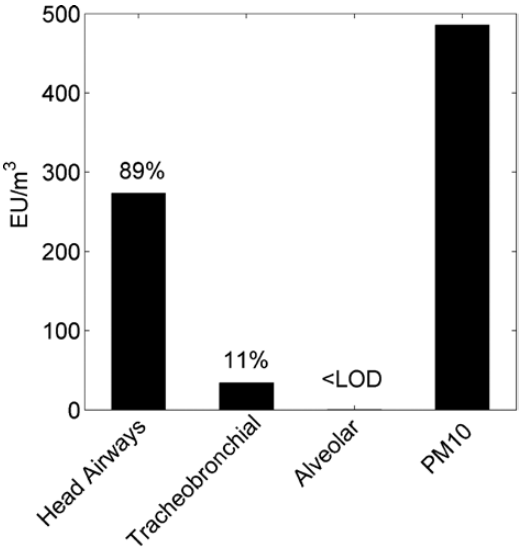

Fig. 5. Regional deposition of endotoxin reported in endotoxin units per cubic meter of air. The percentages above the bars represent the proportion of endotoxin depositing in each region. Regional deposition is compared to the total amount of endotoxin measured by a PM_{10} sampler.

percentage of endotoxin depositing in each region is listed above the bars. As expected, most of the airborne endotoxin was estimated to deposit in the head airways since the endotoxin is likely to be concentrated primarily in the larger particles (diameter > 0.5 μm; Kujundzic *et al.*, 2006). A small fraction of the endotoxin penetrated to the tracheobronchial region, but the concentration of endotoxin in the alveolar region was below the limit of detection. The bar on the right shows the concentration of endotoxin measured on the filter of the PM_{10} sampler. The total endotoxin concentration was 1.58 times higher than the concentration that deposits in the respiratory system.

DISCUSSION

The RDS estimates aerosol deposition in the three regions of the human respiratory system. We have validated this device using fluorescence analysis for two aerosol size distributions. By comparing the RDS sampler model with the ICRP model, we can also estimate RDS performance (both regional and total deposition) for a wide range of theoretical size distributions, as shown in Fig. 6. The percent differences between the aerosol mass measured by the RDS and the mass depositing within the respiratory tract are plotted in Fig. 6 as isopleths (hence, 'bias map') as a function of the MMD and the GSD of the aerosol size distribution. The largest biases are predicted for the head airways region when the aerosol MMD is larger than ~0.5 μm. The overestimation is due to the deposition of particles >2 μm in the first foam substrate (assuming particles are aspirated with 100% efficiency). This results in some underestimation in the tracheobronchial and alveolar regions, generally <40%. In locations where large particles are present, it may be necessary to design an inhalable sampling inlet that operates at 16.7 l min^{-1} of flow to prevent oversampling of supermicron particles. Tracheobronchial deposition is also overestimated for very narrow size distributions (with GSD < 2). For aerosol with MMD < 0.5 μm, the magnitude of the bias in any stage was generally <40%. The RDS will perform well for many types of aerosol size distributions resulting from combustion, fumes, mists, and engineered nanoparticles but may be biased for aerosols resulting for grinding or other mechanical processes encountered in the occupational setting (resulting in large aerosol size distributions and an overestimation of dose). The substrates were selected such that the RDS would over-predict the deposition, when a better fit to the ICRP convention was not possible, to provide a conservative estimate of regional deposition. A sampler that estimates PM_{10} concentration is also conservative but has no ability to estimate regional deposition and may overestimate dose (see Fig. 5). Future work should consider the design of an optimized holder (to minimize losses) and characterize aspiration efficiency of the sampler.

Despite the demonstrated accuracy for mass-based measurements, the RDS cannot be used for gravimetric analysis. This is due to large humidity artifacts for the polyurethane foam (Koehler *et al.*, 2009). The limit of detection, defined as five times the standard deviation of repeated weighings of a blank foam substrate, ranged from 0.5 mg for the smallest substrate (foam insert #1) to 3.2 mg for the largest substrate (foam insert #4). When the RDS sampled from the laboratory-generated, smaller size distribution, ~1% of the mass deposited within foam insert #4. Thus, to exceed the gravimetric limit of detection for foam insert #4 and that size distribution, the ambient concentration would need to exceed 40 mg m^{-3} for an 8-h sample, well above existing occupational exposure limits. The screens also are not conducive to gravimetric analysis because the diameter is so large it will not fit within most commercial microbalances. However, other chemical analyses are

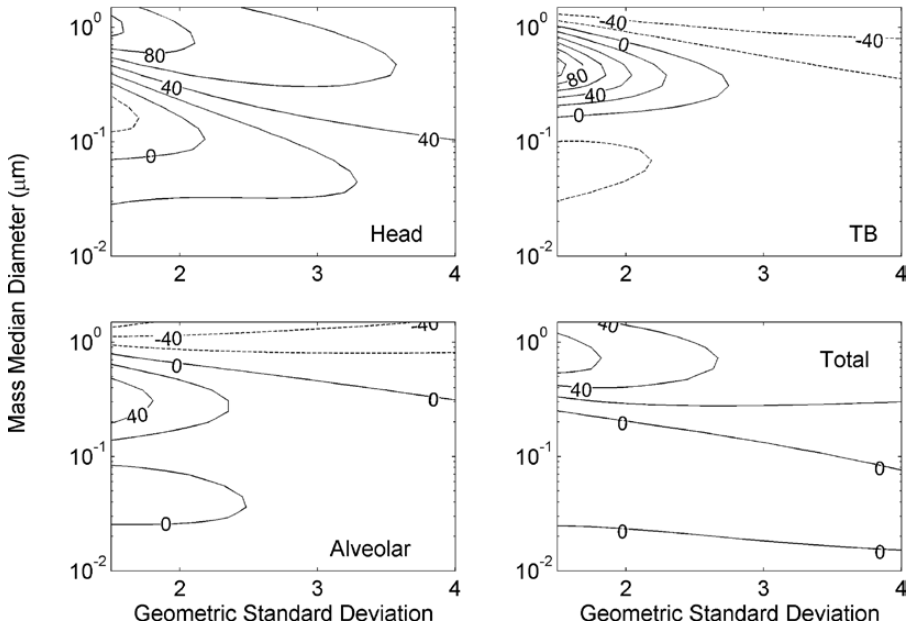

Fig. 6. Theoretical bias map for the error between estimated deposition (RDS sampler model) and assumed regional and total deposition (ICRP model) in the human respiratory tract for varying particle size distributions of unit density spheres.

possible with the RDS substrates (endotoxin, for example, as demonstrated here). Foam substrates have been used for analysis of trace metals (Dillner *et al.*, 2007), polycyclic aromatic hydrocarbons (Maddalena *et al.*, 1998), and semi- and non-polar organic tracer compounds (Sun *et al.*, 2009).

The model described above (equations 1 and 5) could be used to redesign the RDS to match any regional deposition convention of interest. Any fixed flow and fixed geometry sampler will only be able to estimate a single deposition convention and cannot simultaneously estimate all physiologies or breathing conditions. Thus, redesigning the sampler may be useful for future studies considering the deposition of particles among children or adults with altered lung function (e.g. chronic obstructive pulmonary disease) or for heavy exercise conditions where nose breathing may not be appropriate. The RDS could also be redesigned to match the conventions for different breathing conditions described by Bartley and Vincent (2011). Comparing the ICRP convention used here (average of males and females, three exercise conditions) to the six breathing conditions described by Bartley and Vincent (sitting, light exercise, and heavy exercise—with normal and mouth breathing in each case), we found that the ICRP convention yielded deposition fractions generally in the middle of all of these cases for the tracheobronchial region. For the head airways and alveolar regions, our sampler provided a more conservative (high deposition) estimate for deposited mass. The largest differences in size-specific deposition fractions, when considering different breathing conditions, were observed for particle sizes >1 μm or <0.02 μm. Since the RDS is a mass-based sampler, particles <0.02 μm will not contribute substantially to the measured mass for size distributions likely to be encountered in the ambient air or most occupational settings. The polyurethane foam also collects particles larger than ~2 μm with 100% efficiency, regardless of fiber diameter or face velocity, so changes in deposition fraction with breathing conditions for supermicron particles cannot be captured by this sampler. The RDS was designed such that the deposition fractions tend to be somewhat overestimated (protective, see Fig. 1) when a perfect fit to the ICRP convention was not possible. As such, the RDS tends to overestimate the mass (see Fig. 6) and this overestimation may be larger when compared to the breathing conditions considered by Bartley and Vincent (2011). We generated bias maps for the RDS compared to the individual breathing conditions and found that the RDS overestimated the mass to different regions of the respiratory tract by up to 300% compared to the individual breathing conventions, yet rarely underestimated the deposited mass for typical particle size distributions.

The foam and screen deposition models used to predict particle deposition (equations 1 and 5) do not account for electrostatic deposition mechanisms. Additionally, the foam deposition model (equation 1) does not account for interception. Interception is not likely to bias to the RDS because it is explicitly accounted for in equation (5) and may be indirectly accounted for in equation (1), which is based on laboratory measurements of total deposition (see Clark *et al.*, 2009). In the ambient environment, aerosol charge approaches a Boltzmann distribution over time (Liu *et al.*, 1985). As such, few submicron particles have more than four charges and electrostatics should have a negligible effect on particle deposition (recall that supermicron particles are collected with nearly 100% efficiency in the first foam substrate regardless of charging). Particle or substrate charging will lead to increased particle deposition and may bias the RDS. Single-fiber efficiencies for electrostatic forces (E_q) with a neutral fiber and charged particles are small for submicron particles up to the Rayleigh limit of charging ($E_q < 0.05$), with the largest values for the face velocities, such as those in stages 2 and 5 (Hinds, 1999). The influence of charged particles will lead to overestimation of particle mass and will be strongest for highly charged submicron particles. The effect of charged fibers is difficult to quantify (Hinds, 1999) but may be important when sampling at low humidity.

CONCLUSIONS

A RDS has been developed that employs foam and nylon mesh substrates to mimic aerosol deposition in each region of the respiratory tract. These substrates are not amenable to gravimetric analysis due to large humidity biases but are suitable for a variety of chemical analyses. We have demonstrated that the RDS substrates can be extracted to estimate the regional deposition of fluorescent aerosol in the laboratory and endotoxin aerosol in the field. The foam and nylon mesh act as the size selectors and collection substrates, proving a physiologically relevant estimate of deposition in regions of the human respiratory tract.

FUNDING

National Institute for Occupational Safety and Health (NIOSH, R03OH009248); Pilot Project Award from the Mountain and Plains Education and Research Center (T42OH009229).

Acknowledgement—The authors would like to thank Taylor Carpenter for her assistance with the fluorescence analysis.

REFERENCES

Bartley DL, Vincent JH. (2011) Sampling conventions for estimating ultrafine and fine aerosol particle deposition in the human respiratory tract. Ann Occup Hyg; 55: 696–709.

Cena LG, Anthony TR, Peters TM. (2011) A personal nanoparticle respiratory deposition (NRD) sampler. Environ Sci Technol; 45: 6483–90.

Cheng YS, Keating JA, Kanapilly GM. (1980) Theory and calibration of a screen-type diffusion battery. J Aerosol Sci; 11: 549–56.

Clark P, Koehler KA, Volckens J. (2009) An improved model for particle deposition in porous foams. J Aerosol Sci; 40: 563–72.

Dillner AM, Shafer MM, Schauer JJ. (2007) A novel method using polyurethane foam (PUF) substrates to determine trace element concentrations in size-segregated atmospheric particulate matter on short time scales. Aerosol Sci Technol; 41: 75–85.

Hinds WC. (1999) Aerosol technology: properties, behavior, and measurement of airborne particles. New York, NY: Wiley.

ICRP. (1994) Human respiratory tract model for radiological protection. Oxford, UK: Elsevier Science, Ltd.

ISO/CEN. (2012) prEN/ISO DIS 13138. Air quality—criteria for sampling according to particle deposition in the human respiratory system. Geneva, Switzerland: International Organization for Standardization.

Johnson DL, Esmen NA. (2004) Method-induced misclassification for a respirable dust sampled using ISO/ACGIH/CEN criteria. Ann Occup Hyg; 48: 13–20.

Kelly JT, Avise J, Cai C, Kaduwela AP. (2011) Simulating particle size distributions over California and impact on lung deposition fraction. Aerosol Sci Technol; 45: 148–62.

Kenny LC, Aitken RJ, Beaumont G *et al.* (2001) Investigation and application of a model for porous foam aerosol penetration. J Aerosol Sci; 32: 271–85.

Koehler KA, Clark P, Volckens J. (2009) Development of a sampler for total aerosol deposition in the human respiratory tract. Ann Occup Hyg; 53: 731–8.

Kujundzic E, Hernandez M, Miller S. (2006) Particle size distributions and concentrations of airborne endotoxin using novel collection methods in homes during the winter and summer seasons. Indoor Air; 16: 216–26.

Kuo YM, Huang SH, Shih TS *et al.* (2005) Development of a size-selective inlet-simulating ICRP lung deposition fraction. Aerosol Sci Technol; 39: 437–43.

Liu BYH, Pui DYH, Rubow KL *et al.* (1985) Electrostatic effects in aerosol sampling and filtration. Ann Occup Hyg; 29: 251–69.

Maddalena RL, McKone TE, Kado NY. (1998) Simple and rapid extraction of polycyclic aromatic hydrocarbons collected on polyurethane foam adsorbent. Atmos Environ; 32: 2497–503.

Sun QY, Alexandrova OA, Herckes P *et al.* (2009) Quantitative extraction of organic tracer compounds from ambient particulate matter collected on polymer substrates. Talanta; 78: 1115–21.

Tolocka MP, Tseng PT, Wiener RW. (2001) Optimization of the wash-off method for measuring aerosol concentrations. Aerosol Sci Technol; 34: 416–21.